M&C 2017 - International Conference on Mathematics & Computational Methods Applied to Nuclear Science & Engineering, Jeju, Korea, April 16-20, 2017, on USB (2017)

Continuous-energy perturbation calculations using Taylor series expansion in the MORET code

Alexis Jinaphanh*, Nicolas Leclaire*

* *Institut de Radioprotection et de sûreté nucléaire (IRSN), PSN-EXP/SNC/LNC*
BP 17, 92262 Fontenay-aux-Roses, France
alexis.jinaphanh@irsn.fr, nicolas.leclaire@irsn.fr

Abstract - *The MORET code, developed at IRSN (Institut de Radioprotection et de Sûreté nucléaire), is a simulation tool that solves the transport equation for neutrons using the Monte Carlo method. Recently have been implemented the perturbation procedure using first order Taylor series expansion in the continuous-energy calculation relying on the estimation of sensitivity coefficient to isotopic concentrations which have been recently implemented in the MORET code. Thus, the MORET code now offers the users the possibility to use either the correlated sampling or taylor series methods to estimate perturbations. The present paper describes the continuous-energy perturbation method based on the Taylor series expansion which have been implemented in the last release of the code. In addition, some considerations about the implementation and the verification are presented. The verification has been performed using several ICSBEP and OECD/NEA benchmarks and some configurations of the french proprietary experimental program MIRTE.*

I. INTRODUCTION

The MORET code [1] is a simulation tool that solves the transport equation for neutrons using the Monte Carlo method. Initially designed to perform calculations to support criticality safety assessments, the multigroup version of the code is still a key component of the "standard route" of the French criticality calculation package called CRISTAL [2]. The MORET code is developed at the Institut de Radioprotection et de Sûreté Nucléaire (IRSN) and has also been widely used for the design and evaluation of experimental programs, as for example the french proprietary program MIRTE [3].

In this framework, one of the tasks is to evaluate experimental uncertainties through perturbation calculations. Several approaches can be adopted in order to estimate the effect, on k_{eff}, of a perturbation. The most obvious one consists of performing two separate calculations. However, the effect of a small perturbation may be difficult or, frequently, impossible to calculate directly because the inherent statistical uncertainty in the calculation may be larger than the effect of the perturbation itself. It is also well known that performing a couple of simulations, one for the initial system and one for the perturbed system, is not the best solution in terms of computation time (indeed, the variation can be determined accurately only if the two calculations are sufficiently converged).

Perturbation methods allow calculating easily, accurately and without an important increase of the computation time, the k_{eff} difference (Δk_{eff}) due to small perturbations on the data, especially material densities and isotope concentrations. Such calculations may be used in a wide range of applications from the calculation of experimental uncertainties to the estimation of the neutron effective lifetime. Mainly two perturbations methods have been developed for Monte Carlo calculations [4, 5, 6] : correlated sampling and differential operator sampling. The first one has been implemented in the early 2000 in the multi-group calculation route of the MORET code embedded in the CRISTAL package [7, 8] and has been adapted to continuous-energy physics in the late 2000. With the recent implementation of the Taylor series expansion perturbation method based on the differential operator sampling, the 5.D.1 release of the MORET code now embeds two different methods for perturbation calculations.

The present paper describes the theory, the implementation and the verification on several configurations of the Taylor series expansion perturbation capability.

II. THEORY

In the implementation of this feature, a perturbation on the density of a material has been considered equivalent to homogeneous perturbations on concentrations of isotopes contained in this material. Thus, only perturbations to concentrations are described in this paper.

1. Taylor series expansion perturbations

The first order Taylor series expansion can be expressed as equation (1).

$$\Delta k_{eff} = k_{eff}(\alpha + \Delta\alpha) - k_{eff}(\alpha) = \sum_i \alpha_i \frac{\partial k_{eff}}{\partial \alpha_i} \frac{\Delta \alpha_i}{\alpha_i} \qquad (1)$$

Here α_i denotes the concentration for isotope i and $\alpha = (\alpha_i)_{i\in[1,n]}$ a set of concentrations. Thus, the estimation of the k_{eff} difference relies on the Monte Carlo estimation of (2), which can be also written as k_{eff} times a sensitivity coefficient (S_{α_i}) with respect to the concentration α_i.

$$\alpha_i \frac{\partial k_{eff}}{\partial \alpha_i} = k_{eff} \frac{\alpha_i}{k_{eff}} \frac{\partial k_{eff}}{\partial \alpha_i} = k_{eff} S_{\alpha_i} \qquad (2)$$

Recently, a sensitivity coefficient calculation capability has been developed in the MORET 5 code using the differential operator method [9, 10].

2. Sensitivity coefficient to isotope's concentrations

The cycle wise estimation k_0 of k_{eff} is built using random contributions ξ_j through the relationship (3). If not specified,

one may consider to be in a given cycle and omit the cycle index.

$$k_0 = \sum_{j=1}^{\infty} p_j \xi_j \tag{3}$$

Where j is the neutron index in the current cycle, ξ_j is the random contribution of neutron j for the absorption estimator of k_{eff} (4) and p_j is the probability of realization of history j, which can be explicitly written in terms of probabilities describing elementary events of neutron history (5).

$$\xi_j = \frac{\nu\sigma_f(x_N)}{\sigma_a(x_N)} \tag{4}$$

$$p_j = \frac{Q_0(\mathbf{r}_0)}{4\pi}\mathcal{F}(E_0' \to E_0)\mathcal{T}(x_0 \to x_1)\times \prod_{n=1}^{N-1}\mathcal{K}(x_n \to x_{n+1})a(x_N) \tag{5}$$

where Q_0 is the spatial term of the source distribution, $\mathcal{F}$ is the fission spectrum kernel, $\mathcal{T}$ is the transport without collision kernel, $\mathcal{K}$ is the transport kernel defined as $\mathcal{K} = C\mathcal{T}$ where C is the collision kernel and a is the absorption kernel.

It may be noticed that, except for the fission source, all operators have analytic expressions with respect to concentrations.

Expressions of random contributions are needed whenever a response is desired. This means that derivatives of k_{eff} have to be expressed as a response, i.e. similar to equation (3). The main idea of this differential operator method is to partially differentiate contributions to the k_{eff} estimator in order to get an estimator for partial derivatives. Hereafter, the prime refers to partial differentiation with respect to α_i with α_i being a concentration. Differentiating (3) gives equation (6).

$$k_0' = \sum_j p_j \mu_j \tag{6}$$

with μ_j given in (7).

$$\mu_j = \left[\frac{Q_0'(\mathbf{r}_0)}{Q_0(\mathbf{r}_0)} + \frac{\mathcal{F}'(E_0' \to E_0)}{\mathcal{F}(E_0' \to E_0)} + \frac{\mathcal{T}'(x_0 \to x_1)}{\mathcal{T}(x_0 \to x_1)} + \sum_{n=1}^{N-1}\frac{\mathcal{K}'(x_n \to x_{n+1})}{\mathcal{K}(x_n \to x_{n+1})} + \frac{a'}{a} + \frac{\xi_j'}{\xi_j}\right]\xi_j \tag{7}$$

If the random contribution μ_j can be expressed and evaluated, it allows reconstructing an estimation of k_0'. As all operators have analytic expressions with respect to concentration except for the fission source Q_0, the derivatives of these kernels can be written explicitly. So, the random contribution will be divided into the fission source derivatives and what is explicitly dependant of concentrations (denoted μ_0). Rewriting equation (7) in this sense gives (8).

$$\mu_j = \left(\frac{Q_0'(\mathbf{r}_0)}{Q_0(\mathbf{r}_0)} + \mu_0\right)\xi_j \tag{8}$$

Inserting equation (8) in expression (6) gives expression (9).

$$k_0' = \sum_j p_j \left[\frac{Q_0'(\mathbf{r}_0)}{Q_0(\mathbf{r}_0)} + \mu_0\right]\xi_j \tag{9}$$

As a conclusion, the differential operator method allows the construction of random contribution for estimating the derivative of k_{eff} with respect to concentration α_i. This random contribution can be written explicitly except for the fission source term.

It has been demonstrated that the estimation of the fission source derivatives can be replaced (for the first order derivative) by the estimation of the adjoint source [11]. This leads to expression (10) for evaluating the k_0 sensitivity to the concentration α_i.

$$S_{\alpha_i} = \frac{\alpha_i}{k_0}\frac{\partial k_0}{\partial \alpha_i} = \frac{\sum_j p_j \alpha_i \mu_0 \xi_j Q^+(\mathbf{r}_N)}{\sum_j p_j \xi_j Q^+(\mathbf{r}_N)} \tag{10}$$

Where j is the neutron index in the current cycle, ξ_j is the random contribution of neutron j for the absorption estimator of k_{eff}, p_j is the probability of realization of history j, which can be explicitly written in terms of probabilities describing elementary events of neutron history. Finally, $Q^+(\mathbf{r}_N)$ is the adjoint source at the location $\mathbf{r}_N$ and μ_0 is a random contribution term described in equation (11).

$$\mu_0 = \sum_{n=1}^{N} -\sigma_t^i(E_n)\ell(\mathbf{r}_n, \mathbf{r}_{n+1})\delta(m) + \sum_{n=1}^{N}\frac{1}{\alpha_i}\delta(m)\delta(i) \tag{11}$$

Here, σ_t^i is the total cross section of isotope i, $\ell(\mathbf{r}_n, \mathbf{r}_{n+1})$ is the distance between collisions n and $n+1$, δ is the Dirac's function, m is the identifier of the material where the event takes place (either transport or collision), $\ell(\mathbf{r}_n, \mathbf{r}_{n+1})$ is the distance between collisions $\mathbf{r}_n$ and $\mathbf{r}_{n+1}$.

During each cycle, sensitivity coefficients to all perturbed concentrations are calculated. Then, at the end of each cycle, sensitivity coefficients are weighted by the concentration's relative variation in order to construct a Δk_{eff} estimation as defined in equation (1).

3. Iterated Fission Probability

The adjoint source can be linked to the adjoint flux $\phi^+(x)$ using the relation (12) where the brackets denotes integration over its subscripts.

$$Q^+(r) = \left\langle \frac{1}{4\pi}\chi(x)\phi^+(x)\right\rangle_{E,\mathbf{\Omega}} \tag{12}$$

A quantity proportional to the adjoint flux can be accessed by simulating L independent random super-histories (neutrons and their progeny), each of them consisting of simulating M generations. Here, L is the number of realization for the Monte Carlo estimation of the adjoint flux at location x. For practical and implementation reasons, L is set to one in our implementation. In the following of this paper, we will denote "dummy" the neutrons that are simulated to estimate the adjoint

source only and "active" the neutrons that may contribute to tallies.

The simulation of a dummy neutron and its progeny over M generations will yield

$$\frac{1}{k_0^M}\prod_{m=1}^{M}\frac{\nu^i\sigma_f^i(z_m)}{\sigma_a^i(z_m)} \tag{13}$$

neutrons where z_m is the absorption site of progeny m. In this model a single dummy neutron is simulated in each generation m and the production rate is accumulated over generations, meaning that the simulated neutron carries all the weight of the progeny. The index i represents the nuclide in which the neutron undergoes an absorption, which may be different for the M generations. In this case, k_0^M is a preset constant (for this cycle) and will be eliminated by the normalization factor. Thus, there is no need to take it into account in equations and tallies. So, the estimation of the adjoint flux is

$$\phi^+(x) \sim \prod_{m=1}^{M}\frac{\nu^i\sigma_f^i(z_{l,m})}{\sigma_a^i(z_{l,m})} \tag{14}$$

Now the adjoint source has to be estimated, i.e. estimates equation (12). It can be done by emitting fission neutron at $\mathbf{r}_N$ with random energy, according to the fission spectrum, and angle, which is Monte Carlo integration. The algorithm implemented in the MORET code for estimating the adjoint source is described in the following section and depicted in figure 1.

III. IMPLEMENTATION

In the context of a perturbation using Taylor series expansion, for all perturbed elements, an estimation of the sensitivity coefficient with respect to the concentration is calculated. Then, at the end of each cycle, it is multiplied by a consistent cycle wise estimation of k_{eff} and the relative variation of the different perturbed systems. Then, using formula (1), the Δk_{eff} is calculated at every cycle. Finally, the averages and the standard deviations of each perturbed systems are updated.

The only random contribution calculated along the simulation of the neutron random walk is the contribution to the sensitivity coefficient with respect to the concentration.

First, when the neutron crosses the material that undergoes a perturbation, the transport process provides non-null random contributions. It is the total macroscopic cross section times the length travelled by the neutron.

Then, the collision process may provide non-null random contributions when the collided nuclide is the one that undergoes a perturbation in the current material or when this material undergoes a density perturbation.

During its life, the neutron will contribute to sensitivity coefficients to all isotopes of materials it crosses and isotopes it collides in media. At its absorption, the adjoint source $Q^+(\mathbf{r}_N)$ has to be tallied. This is done by tallying the absorption estimator of the production, then making a "dummy" neutron born at the current location and following its progeny over several generations. For each death of a "dummy" neutron (neutron used for estimating the adjoint flux only), the absorption estimator of the production is tallied. If any of the progeny dies in a non-fissile nuclide or leak out of the system, the contribution of the active neutron is null. Otherwise, the contribution of the active neutron is multiplied by the $\xi(\mathbf{r}_N)Q^+(\mathbf{r}_N)$ term and added to contributions to sensitivity coefficients for the current cycle. In fact, all the progeny is not simulated but only one neutron per generation and their production rate is accumulated, meaning that one neutron carries all the weight of the generation. Figure 1 illustrates the algortihm for the estimation of the adjoint source.

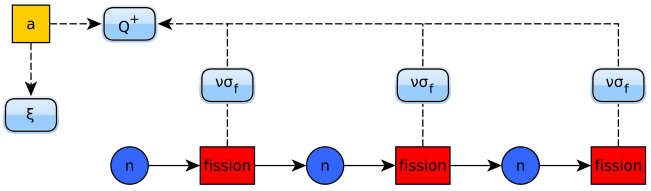

Fig. 1. Algorithm for the estimation of the adjoint source

In this figure, a represents the absorption of an active neutron, n represents the simulation of a dummy neutron. It should be noted that if a dummy neutron is absorbed by a non-fissile nuclide or leaks out of the system, the estimation of $Q^+(\mathbf{r}_N)$ is null.

The user interface has been built around the notion of perturbed system, which is a system where one or several elements, isotope's concentration or material's density, undergo a perturbation. These elements can be either the concentration of an isotope in a material or the density of a material associated with a perturbation value. There is no upper limit for the number of perturbed elements or the number of perturbed systems.

The perturbation using Taylor series expansion has been built following a matrix formalism. In this context, rows are elements that undergo a perturbation along with their perturbation (as relative variations) values according to perturbed systems. Columns are perturbed systems and contain their respective perturbed elements. Elements are identified though their materials using the keyword `MEDI` followed by the isotope's identifier or the `DENS` keyword which designates the density.

```
TAYL nelem npert
    MEDI name isotope1 c_1 c_2 ... c_npert
    MEDI name DENS     c_1 c_2 ... c_npert
    (repeated nelem times)
```

where `nelem` is the number of perturbed elements, `npert` is the number of perturbed systems, `c_i` is the relative variation of concentration (or density) and `name` is the identifier of the material in the geometry.

The user interface of this feature allows constructing several independent perturbations in the same calculation. It has been constructed as a matrix

IV. PRELIMINARY VERIFICATION

The preliminary verification has been performed on two OECD benchmarks and some MIRTE configurations [3] . The verification has been performed using comparisons with the Correlated Sampling procedure as implemented few years ago

in the MORET code and direct perturbation which uses two separate calculations. The following notations are used: "Taylor" stands for the perturbation using Taylor series expansion, "C.S." represents the Correlated Sampling procedure and "ref" is used for direct perturbation.

Results are provided as Δk_{eff} within tables with the corresponding perturbation, where all Δk_{eff} are provided in pcm (1pcm = 0.00001). In addition, absolute standard deviations σ are provided.

1. OECD/NEA Burn-up Credit pin cell benchmark

The investigation of burn-up credit for different types of fuel is an ongoing objective of the NEA-OECD Burn-Up Credit (BUC) expert group of the Working Party on Nuclear Criticality Safety (NEA - WPNCS), which proposed a benchmark based on a pin cell case [12]. This model, displayed in figure 2, is representative for an infinite medium and provides information about reactivity and fuel inventory as a function of burn-up.

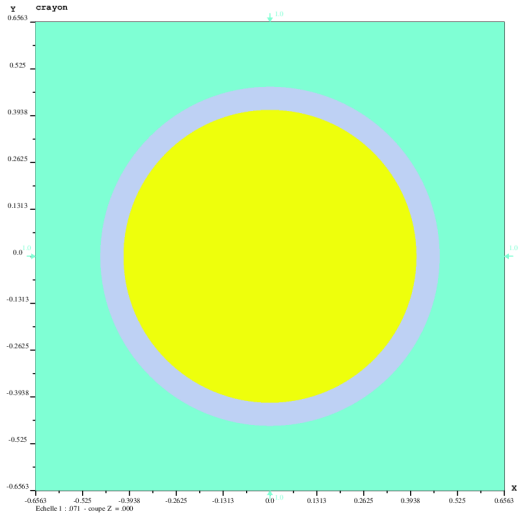

Fig. 2. Burn-Up Credit pin cell configuration at altitude z=0

In order to get accurate results for the direct perturbation, calculations were performed with a 5 pcm standard deviation for this method. Table I displays the Δk_{eff} due to the perturbation of either ^{239}Pu,^{241}Pu,^{238}U concentrations or water density. The results highlight a very good agreement between the different methods, the results being consistent between the several methods. Indeed, all perturbation methods are consistent with each other in the sense that three σ confidence intervals overlap.

These calculations validate the implementation of the Taylor series expansion perturbation method for the present configuration. In addition, it may be noticed that Correlated Sampling computations seem to provide a lower standard deviation than Taylor calculations.

2. OECD/NEA UACSA benchmark

Under the guidance of the OECD/NEA Working Party on Nuclear Criticality Safety (WPNCS), the Expert Group on

Quantity	relative variation	Taylor ($\pm\sigma$)	C.S. ($\pm\sigma$)	ref ($\pm\sigma$)
^{239}Pu	-0.03	-416.3 ± 1.1	-418.1 ± 0.8	-430.6 ± 9.2
^{239}Pu	0.01	138.8 ± 0.4	137.1 ± 0.3	121.1 ± 9.0
water density	0.01	174.4 ± 1.6	172.4 ± 1.1	158.8 ± 9.0
^{241}Pu	0.03	181.4 ± 0.6	182.2 ± 0.4	175.3 ± 9.1
^{238}U	-0.01	113.6 ± 0.7	113.6 ± 0.5	102.2 ± 9.1

TABLE I. Δk_{eff} calculations (in pcm) due to variations for the burn-up Credit benchmark

Uncertainty Analyses for Criticality Safety Assessment (EG UACSA) proposed a benchmark [13], which aims at providing common models for the comparison of sensitivity calculation capabilities from several software packages. Although the benchmark is made of three test cases, this paper presents the results obtained for the detailed model of Phase III.1 only. This case consists of a square lattice of Mixed Plutonium-Uranium Oxide Pins containing 19.7 wt. % of plutonium out of which 11.5 wt. % was ^{240}Pu. This configuration represents a reprocessed fast reactor fuel assembly in a shipping cask for an accidental scenario where water fills the cask. It is based on the benchmark model that can be found in the International Handbook of Evaluated Criticality Safety Benchmark Experiments (referred to as ICSBEP Handbook) under the identifier MIX-COMP-THERM-001-001 [14].

The fuel pins model consists of a clad of diameter 0.5842 cm, a gap of diameter 0.508 cm and the MOX fuel of diameter 0.49403 cm and the pin's height is 91.44 cm. The array of pins consists of 28 (17 for the upper row) × 22 identical pins for a total of 605 pins with a square pitch of 0.9525 cm. The top and bottom of the pins are modeled by a homogenized material. Figure 3 displays the detailed configuration of the phase III at altitude z=0.

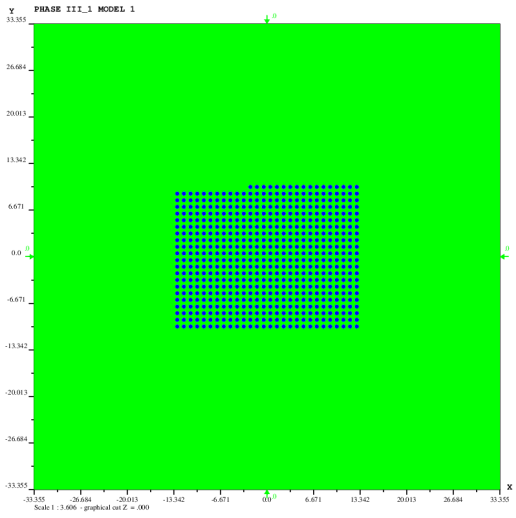

Fig. 3. UACSA phase III detailed configuration at altitude z=0

Table II displays results for Δk_{eff} due to several perturbations calculated with Taylor series, Correlated Sampling procedure and a direct perturbation. In addition to the perturbation of single isotopes, a perturbation on water density

and a combination of all previous perturbations are presented. Results for the three perturbation methods show a very good agreement, the 3-σ confidence interval overlapping.

Quantity	relative variation	Taylor($\pm\sigma$)	C.S.($\pm\sigma$)	ref($\pm\sigma$)
^{239}Pu	0.01	117.9 ± 0.5	118.5 ± 0.2	104 ± 11
^{238}U	0.03	-28.7 ± 1.3	-28.1 ± 0.6	-39 ± 11
^{235}U	-0.02	-4.8 ± 0.1	-4.6 ± 0.0	-15 ± 11
^{240}Pu	-0.05	267.6 ± 0.6	271.0 ± 0.3	240 ± 11
water density	0.01	399.5 ± 2.5	400.2 ± 0.4	394 ± 11
combination		751.5 ± 2.8	756.0 ± 1.7	765 ± 11

TABLE II. Δk_{eff} calculations (in pcm) due to relative variations

This enhances the validation of the implementation of the Taylor series expansion perturbation method for the presented configurations. Again, Taylor based perturbations have a higher standard deviation than the Correlated Sampling procedure results.

3. The MIRTE program

The third verification is extracted from the MIRTE (Materials in Interacting and Reflecting configurations, all Thicknesses) program [3] designed with the aim to validate a list of structural materials representative of the industrial configurations encountered within the fuel cycle.

A. Description of the MIRTE experiments

This program was initiated in 2005 by IRSN and carried out from 2008 to 2013 at the CEA Valduc Centre (France) on the Apparatus B assembly, which is a subcritical experimental facility that has been used for 50 years by IRSN for criticality experimental programs.

In the nomenclature of the MIRTE experiments, the identifier of the configuration takes into account the number of lattices of rods (1A, 2A, 4A), the type of material, and its thickness. For instance, for interacting configurations with 5-mm titanium plates between four lattices of UO_2 rods, the identifier is 4A-Ti-005.

Figure 4 shows the three types of configurations performed during the phase 1, 2.1 and 2.2 of the MIRTE program.

Reflected configurations consist of one UO_2 rod lattice reflected on all four sides by the test screens (see Fig. 4-a). The four screens are maintained in position by four aluminum devices. The lower and upper grids are designed for each reflected configuration in order to ensure a distance of 0.8 cm (half of the lattice pitch value) between the center of the outermost rods and the inside surface of the test screens. In this application, the configuration with Aluminium as the tested material is used for verification. The perturbation capability is tested on density of the Aluminium block, density of the UO_2 pellets, impurities of the tested block and isotopics of Uranium in UO_2 rods. The evaluation of the impact of isotopics is performed by modifying the ^{235}U concentration compensated by an adjustment of the ^{238}U isotope content to preserve normalisation.

The experimental device presented in Fig. 4-b involves two UO_2 rod lattices separated by a large screen with a thickness ranging from 5 to 30 cm. It consists of two movable aluminum (AG3) baskets composed of two grids pierced by 10×62 holes to allow the rods to be installed in a rectangular lattice. The grids are designed to ensure a distance of 0.8 cm between the center of the outermost rods and the external surface of the test screen. Thus, no gap is considered between the outer edge of the grid maintaining the rods and the test screen. Among these configurations, the experiment involving a Rhodium solution in a Zircaloy box has been used to perform the calculations. Here, the perturbation capability is tested on density of the Rhodium solution, density of the UO_2 pellets and isotopics of UO_2 rods.

Figure 4-c presents the experimental device, which is composed of four movable aluminum baskets. The square grids are pierced by 15×15 holes. A dedicated aluminum device was manufactured to maintain the plates all along the height. As for the previous configurations, a distance of 0.8 cm between the center of the outermost rods and the surface of the cruciform plates is considered. Three cases were used within this series to perform test on perturbation calculations. Configurations involved screens made of Molybdenum, Titanium and Manganese. Perturbation on the density of the tested materials, density of UO_2 pellets and the isotopics are considered.

B. Results

The MIRTE experimental program being a proprietary program, k_{eff} results cannot be used for publication. So, values provided in this section are Δk_{eff} due to a modification of 1% of a concentration or density. For isotopics, a variation of 0.05% of ^{235}U compensated by a variation of ^{238}U is applied. The variation responsible for the k_{eff} variation does not correspond to the correct experimental uncertainties which are lower.

Calculations were performed with the same parameters (number of neutrons per cycles, active cycles and inactive cycles) for all configurations.

Table III shows results of the perturbation calculation on the configuration with Aluminium as tested material.

configuration	Quantity	Taylor($\pm\sigma$)	C.S.($\pm\sigma$)
1A-Al-200	Density Al (1%)	-73 ± 1.46	-78 ± 0.91
	Density UO_2 (1%)	151 ± 2.26	149 ± 1.06
	Impurities block Al (100%)	126 ± 2.00	134 ± 2.00
	Isotopics UO_2 (0.05%)	-13.1 ± 0.09	-12.9 ± 0.05

TABLE III. Δk_{eff} on 1A MIRTE experiments

This first configuration shows a very good agreement between the Correlated Sampling and Taylor series expansion perturbation methods. Three σ confidence interval overlap for all changes in the density and compositions. This suggests that the implementation of the Taylor based perturbation method is correct in the MORET code. It may be noticed that Correlated Sampling provides lower standard deviations on average of a factor 2.

Table IV displays results for the configuration involving a Rhodium sulphate solution in a Zircaloy box.

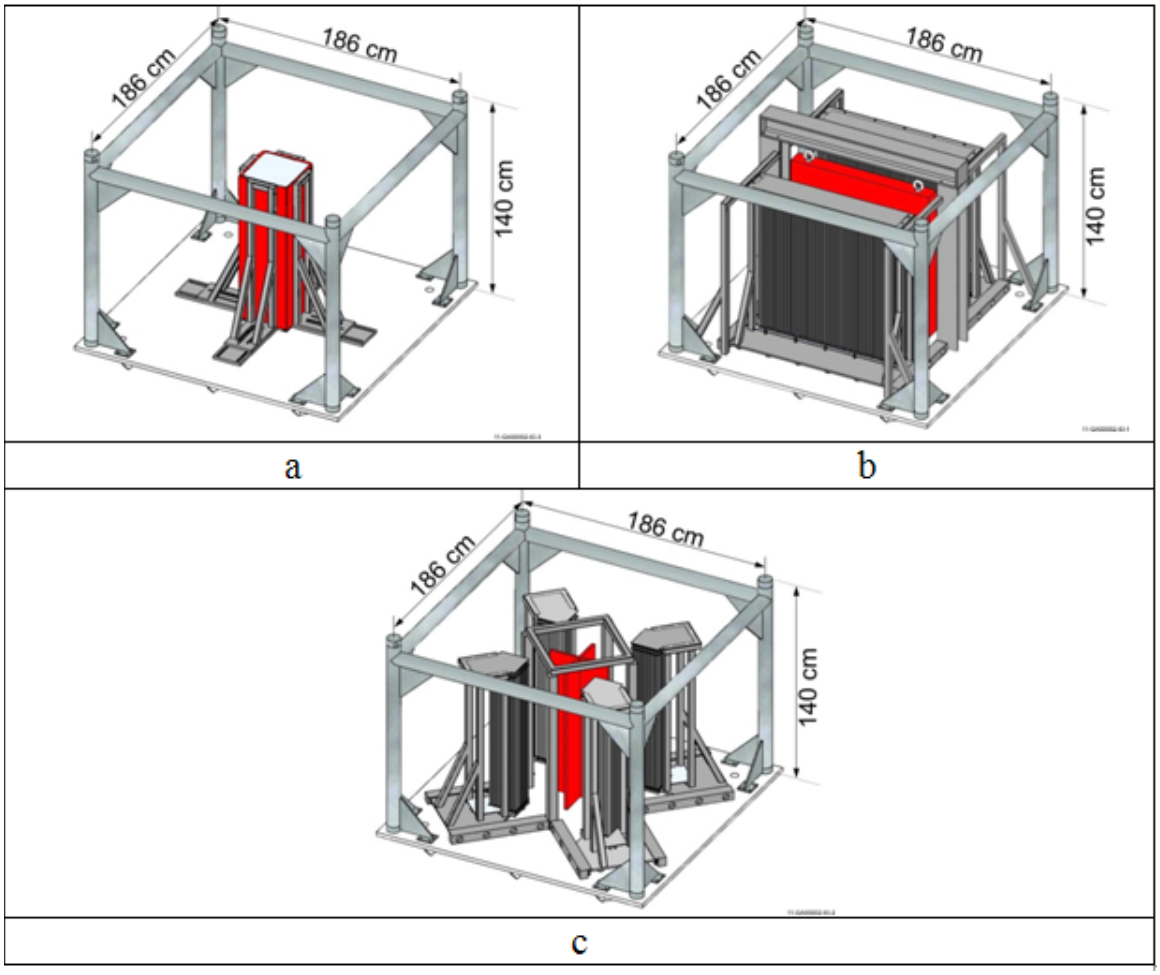

Fig. 4. Experimental device for the three types of configurations

configuration	Quantity	Taylor ($\pm\sigma$)	C.S. ($\pm\sigma$)
2A-Rh-040	Density Rh (1%)	-82 ± 2.71	-77 ± 1.41
	Density UO_2 (1%)	145 ± 2.41	142 ± 1.15
	Isotopics UO_2 (0.05%)	-13.4 ± 0.09	-13.3 ± 0.04

TABLE IV. Δk_{eff} on 2A MIRTE experiments

This configuration highlights a very good agreement between the two methods, confidence intervals overlapping for all changes in the density and compositions.

Table V shows results of the configurations involving screens made of Molybdenum, Titanium and Manganese.

These three test cases highlight a very good agreement between the two methods, confidence intervals overlapping for all changes in the density and compositions of all configurations.

Finally, the calculations performed on the MIRTE experimental program show a good agreement between the Correlated Sampling procedure and the Taylor series expansion method.

configuration	Quantity	Taylor ($\pm\sigma$)	C.S. ($\pm\sigma$)
4A-Mo-010	Density Mo (1%)	-40 ± 1.0	-40 ± 0.5
	Density UO_2 (1%)	155 ± 2	155 ± 0.9
	Isotopics UO_2 (0.05%)	-13.8 ± 0.10	-13.7 ± 0.04
4A-Ti-005	Density Ti (1%)	-37.7 ± 0.5	-37 ± 0.2
	Density UO_2 (1%)	161 ± 1.5	160 ± 0.7
	Isotopics UO_2 (0.05%)	-13.9 ± 0.10	-13.8 ± 0.04
4A-Mn-020	Density Mn (1%)	-60 ± 1.6	-57 ± 0.9
	Density UO_2 (1%)	161 ± 2.2	161 ± 1.1
	Isotopics UO_2 (0.05%)	-14 ± 0.09	-14 ± 0.05

TABLE V. Δk_{eff} on 4A MIRTE experiments

4. Performance

In this section, some considerations on performances are presented. However, it should be mentioned that the perturbation using Taylor series expansion in MORET is a recently developed capability. Thus, no optimization has been performed on the storage model or on computation time. So, performances described here are for information only and might strongly differ in stable and optimized releases.

Performances are compared to performances of the Correlated Sampling method. They are also compared to a reference calculation, i.e. a calculation without any perturbation, which enables us to estimate the increase in memory usage and computation time due to perturbations. Obviously, all calculations are performed with similar stopping criteria that is a given standard deviation on the k_{eff}.

Computation time and memory footprint for the configurations used in the validation process are displayed in table VI. Computation time is the one provided in the output file of the code and the memory footprint relies on the Resident Set Size (RSS) of the "ps" Linux command. Calculations have been performed on a Intel(R) Xeon(R) CPU X5460 @ 3.16GHz processor, with 31 GB of RAM on a Linux CentOS 6.6 operating system.

case	method	number of perturbations	Computation time (min)	Memory footprint (MB)
BUC	Taylor	29	385.9	343.5
	C.S.	29	1656.3	771.4
	reference	0	151.5	343.3
UACSA	Taylor	6	769.7	540.8
	C.S.	6	1090.2	705.5
	reference	0	543.7	540.4

TABLE VI. Performance

This table highlights that, for a perturbation using Taylor series, the increase in memory usage is very low (less than 1MB) and the increase in computation time is quite low. For the correlated sampling, the computation time is multiplied by a factor of 5 to 10 and the memory usage is multiplied by a factor of 2 but, as shown in previous sections, leads to lower standard deviations.

The Correlated sampling procedure as implemented in the MORET code relies on the construction of several macroscopic cross section sets, each set corresponding to a perturbed system. Thus, it leads to an important increase in terms of memory usage with the increase of the number of perturbed systems. Furthermore, for continuous energy, the number of interpolations in the energy grid is proportional to the number of perturbed system since the weight correction in the Correlated Sampling procedure requires the estimation of the cross section.

On the contrary, the perturbation using Taylor series expansion first computes the derivatives of k_{eff} to isotopic concentrations of isotopes involved in the perturbed systems and then reconstruct the perturbation. Thus, the increase in memory usage is quite low. On the other hand, the increase in computation time is rather constant since, independently of the number of perturbations (either perturbed elements or perturbed systems), the additionnal computation time is essentially due to the simulation of dummy neutrons at each absorption point.

All these elements suggest a more important increase in computation time and memory usage for the Correlated Sampling compared to Taylor series expansion perturbations, when the number of perturbed systems increase. However, it has been noticed, for calculations not presented here, that when there is only one perturbed systems with numerous perturbed elements, the Correlated sampling seems more efficient in terms of computation time.

V. CONCLUSIONS

A continuous energy perturbation capability using Taylor series expansion has been successfully implemented in the MORET code. It relies on the computation of adjoint weighted sensitivity coefficients with respect to isotopic concentrations. Sensitivity coefficients are computed using the differential operator method and an estimation of the adjoint source in order to take into account correlations between cycles.

The continuous energy route of the MORET code now embeds two different methods, Correlated Sampling and Taylor series expansion, for estimating the effect on k_{eff} of a perturbation on the isotope's concentration or on material density. The Taylor series approach relies on the calculation of sensitivity coefficients with respect to the concentration of different isotopes providing the slope corresponding to the perturbation. Then, these coefficients are combined with variations of parameters and altogether to provide an estimation of the Δk_{eff}.

Verification has been performed on several configurations showing good results. All results display a very good agreement between both methods as confidence intervals overlap. On the presented cases, the Taylor based perturbation capability appears much more efficient in terms of computation time and memory usage than the Correlated Sampling when several independent perturbations are calculated. However, the Correlated Sampling calculations have a lower standard deviations than the Taylor based perturbations of a factor, on average for these configurations, lower than 2.

As a future work, it is first planned to improve the user interface and optimize performance. In addition, it is foreseen to extend the verification database of the Taylor perturbation capability, then, it is planned to perform studies on the validity domain of the Taylor method.

The computation of sensitivity coefficients to isotopic concentration relies on the Iterated Fission Probability (IFP). However, as implemented in the MORET code, the IFP method may lead to an increase in computation time and provide a high standard deviation in some configurations. In order to mitigate these effects, an alternate approach to the simulation of "dummy" neutrons has been recently implemented in the MORET code based on the CLUTCH approach for the estimation of the adjoint source. It consists of estimating the average progeny for a geometrical mesh during inactive cycles and then use this approximation instead of simulating "dummy" neutrons. This reduce the computation time and the variance associated to the estimation of sensitivity coefficients. It is planned to apply this approach to the calculation of sensitivity coefficients used in the Taylor series expansion perturbation method.

Finally, it is planned to adapt the Taylor perturbation capability to a multigroup calculation within the frame of the CRISTAL French criticality calculation package [2].

REFERENCES

1. B. COCHET, A. JINAPHANH, L. HEULERS, and O. JACQUET, "Capabilities overview of the MORET 5 Monte Carlo code," *Annals of nuclear Energy*, **82**, 74–84 (2015).
2. J.-M. GOMIT, J. MISS, A. AGGERY, C. MAGNAUD, J. TRAMA, and C. RIFFARD, "CRISTAL criticality package twelve years later and new features," in "International Conference on Nuclear Criticality 2011," Edinburgh, Scotland (September 19-22 2011).
3. N. LECLAIRE and AL., "The MIRTE Experimental Program : An Opportunity to Test Structural Materials in Various Configurations in Thermal Energy Spectrum," *Nuclear Science and Engineering*, **01**, *178*, 429–445 (2014).
4. I. LUX and L. KOBLINGER, *Monte Carlo particle transport methods : Neutron and Photon calculations*, CRC Press (1991).
5. H. RIEF, "A Synopsis of Monte Carlo Perturbation Algorithms," *Journal of Computational Physics*, **111**, 33–48 (1994).
6. H. RIEF, "Generalized Monte Carlo perturbation algorithms for Correlated Sampling and a second-order Taylor series approach," *Annals of nuclear Energy*, **11**, *9*, 33–48 (1984).
7. A. LE COCQ, *Contributions au développement des méthodes de Monte-Carlo pour les études de criticité*, Ph.D. thesis, University of Paris XI (1998).
8. J. ANNO, O. JACQUET, and J. MISS, "Validation of MORET 4 Perturbation against Physical Type Fission Products Experiments," in "International Conference on Nuclear Criticality," Tokai-Mura, Japan (October 20–24 2003).
9. A. JINAPHANH, B. COCHET, and N. LECLAIRE, "Continuous energy Sensitivity coefficients in the MORET code," *Nuclear Science and Engineering*, **184**, *01*, 53–68 (2016).
10. A. JINAPHANH, B. COCHET, N. LECLAIRE, and B. QUAGHEBEUR, "Validation of continuous-energy sensitivity coefficients calculation in the MORET code," *ICNC 2015, Charlotte, NC, September 13-17, 2015* (2015).
11. A. BLYSKAVKA, K. RASKACH, and A. TSIBOULIA, "Algorithm of calculation of KEFF Sensitivities to group cross sections using Monte Carlo Method and features of its implementation in the MMKKENO code," *Mathematics and Computation, Avignon, France* (2005).
12. G. J. O'CONNOR AND P. H. LIEM, *Burn-up Credit Criticality Benchmark - Phase IV-B: Results and Analysis of MOX Fuel Depletion Calculations*, Nuclear Energy Agency - Organisation for Economic Cooperation and Development, Paris, France (2003).
13. T. IVANOVA and AL., "OECD/NEA Expert Group on Uncertainty Analysis for Criticality Safety Assessment: Results of Benchmark on Sensitivity Calculation (Phase III)," in "PHYSOR 2012 - Advances in Reactor Physics - Linking Research, Industry, and Education," Knoxville, Tennessee, USA (April 15-20 2012).
14. OECD NUCLEAR ENERGY AGENCY, *ICSBEP Handbook*, report NEA/NSC/DOC(95)03 (2011).